ORIGINAL ARTICLE

An overview of methods of left and right foot motor imagery based on Tikhonov regularisation common spatial pattern

Jiakai Zhang[1] · Xuemei Wang[1] · Boyang Xu[1] · Yan Wu[1] · Xiongjie Lou[1] · Xiaoyan Shen[1,2]

Abstract

The motor imagery brain–computer interface (MI-BCI) provides an interactive control channel for spinal cord injury patients. However, the limitations of feature extraction algorithms may lead to low accuracy and instability in decoding electroencephalogram (EEG) signals. In this study, we examined the classification performance of an MI-BCI system by focusing on the distinction of the left and right foot kinaesthetic motor imagery tasks in five subjects. Feature extraction was performed using the common space pattern (CSP) and the Tikhonov regularisation CSP (TRCSP) spatial filters. TRCSP overcomes the CSP problems of noise sensitivity and overfitting. Moreover, support vector machine (SVM) and linear discriminant analysis (LDA) were used for classification and recognition. We constructed four combined classification methods (TRCSP-SVM, TRCSP-LDA, CSP-SVM, and CSP-LDA) and evaluated them by comparing their accuracies, kappa coefficients, and receiver operating characteristic (ROC) curves. The results showed that the TRCSP-SVM method performed significantly better than others (average accuracy 97%, average kappa coefficient 0.91, and average area under ROC curve (AUC) 0.98). Using TRCSP instead of standard CSP improved accuracy by up to 10%. This study provides insights into the classification of EEG signals. The results of this study can aid lower limb MI-BCI systems in rehabilitation training.

Keywords Electroencephalogram (EEG) · Kinaesthetic motor imagery (KMI) · Tikhonov regularisation CSP (TRCSP) · Support vector machine (SVM) · Linear discriminant analysis (LDA)

1 Introduction

In recent years, the number of patients with physical disabilities or paralysis has increased rapidly owing to accidents, congenital disabilities, diseases, natural disasters, and other reasons. Patients with spinal cord injury (SCI) or amyotrophic lateral sclerosis (ALS) lose autonomic neuromuscular control. Helping patients improve their self-care ability and restore some motor function has become an important research topic in rehabilitation medicine. Current treatments cannot achieve the full reconstruction of limb movements. However, the developments in

computer technology, and the deepening of brain science research, have led to attempts to establish a completely new communication and control pathway to transmit information and commands to and from the brain. This is the so-called brain–computer interface (BCI) [1–3].

As an important paradigm of BCI, motor imagery (MI) has unique advantages in the rehabilitation training of patients who cannot exercise autonomously. MI does not require real limb movement behaviour but can directly map the user's intention of active movement. Several studies [4–6] have used the physiological patterns caused by different imagined limb motions to classify electroencephalogram (EEG) signals and achieve control of external devices such as prosthetics. Because the area of the cerebral cortex corresponding to lower limb movement is relatively small, classification is a challenging task [7]. Most research studies on MI have aimed to classify the left and right hands. In particular, few studies have focused on the classification of the left and right feet. However, in real life, numerous people who lose foot motor function require more rehabilitation training through MI-BCI to reconstruct their gait movements. Therefore, the realisation

---

Jiakai Zhang and Xuemei Wang contributed equally.

✉ Xiaoyan Shen
  xiaoyansho@ntu.edu.cn

[1] School of Information Science and Technology, Nantong University, Nantong 226019, China

[2] Nantong Research Institute for Advanced Communication Technologies, Nantong 226019, China

of the high-precision classification of intended lower limb motion is an inevitable trend for the future application of MI-BCI technology. Feature extraction methods typically used in MI-BCI systems include wavelet packet transform [8], sample entropy [9], power spectral density [10], and common spatial pattern (CSP) analysis [11, 12]. Pattern classification methods include linear discriminant analysis (LDA) [13, 14], support vector machine (SVM) [15], and neural networks [16, 17]. CSP is extensively used as a representative spatial filtering method owing to its good classification performance [18]. Moreover, some researchers improved the CSP algorithm by increasing its robustness and proposed filter band CSP (FBCSP) [19]. The original EEG signal was divided into multiple frequency bands for band-pass filtering to extract features. Although the classification accuracy was improved, the calculation load increased substantially. Other researchers proposed adaptive CSP (ACSP), substantially reducing the training time of new subjects, and classified MI into three types [20]. Addressing the low signal-to-noise ratio and individual differences in EEG signals, these researchers also proposed an improved B-CSP algorithm to select the best frequency band for each electrode using the Bhattacharyya distance method [21]. To improve the practical performance of EEG-based control paradigm for comprehensive and complex daily situations, Lu et al. proposed an asynchronous artefact-enhanced EEG-based control paradigm assisted by slight facial expression (sFE-paradigm), effectively improving its practical performance [22]. Moreover, limited by the lack of guidelines in model parameter selection and the inability to obtain personal tissue information in practice, EEG modelling in BCI has a gap between the theory and its application. To bridge this gap, Zhang et al. combined the surface EEG simulation with a converter based on the generative adversarial network (GAN) to establish the connection from simulated EEG to its application in BCI classification, remarkably improving the selection results of classifiers [23].

However, CSP has another defect: the method is highly sensitive to noise and prone to overfitting [24]. The regularisation CSP (RCSP) method solves this problem. This study investigated an EEG signal classification algorithm for kinaesthetic motor imagery (KMI). We used a Tikhonov regularisation CSP (TRCSP) filter and an original CSP filter, constructed through OpenViBE (software for BCI) to extract features for 'Move left foot' and 'Move right foot' MI tasks. We then applied both SVM and LDA techniques for classification. Moreover, four combined feature extraction and classification methods, TRCSP-SVM, TRCSP-LDA, CSP-SVM, and CSP-LDA, were established. Classification performance was evaluated using statistical analysis methods (accuracy, kappa value, and receiver operating characteristic (ROC) curve). The best algorithm combination for lower limb KMI classification tasks was then determined.

2 Methods

Our study included EEG signal acquisition, EEG signal processing, and classification performance evaluation. The specific implementation steps are illustrated in Fig. 1. The entire process was implemented using OpenViBE software.

2.1 Subjects, data acquisition, and experimental procedure

Five healthy subjects (S1 ~ S5), three men and two women, aged 22 ~ 24 years, were recruited. Each subject was given sufficient time to familiarise themselves with the signal acquisition equipment and process. This required approximately 30 min, after which the subjects entered the formal data acquisition stage.

OpenBCI (openbci.com, New York) was selected as the EEG signal acquisition device with the sampling frequency set to 250 Hz. Figure 2 shows the electrode placement according to the 10–20 electrode system. The red section represents the electrodes used to obtain the EEG data, and the blue section represents the reference electrodes. Minimising the number of electrodes used for data acquisition simplifies the complexity of data processing and improves real-time efficiency. We selected only the regions most closely related to the cerebral motor sensory cortex (C3, C4, and Cz). Before connecting the electrodes, the scalp was cleaned with medical alcohol, and conductive gel was applied to reduce impedance.

During the experiment, the subjects were asked to perform the KMI task of 'Move left foot' or 'Move right foot' after the prompt icon appeared on the screen. These two tasks are in line with normal human walking gait. Each subject completed 20 groups of tests. There were ten random tasks in each group: 'Move left foot' and 'Move right foot' were performed five times each. The experimental paradigm is shown in Fig. 3. When the cross-mark appeared on the screen, the subject began to focus. After 2 s, the screen displayed an arrow and icon prompting 'Move left foot' or 'Move right foot'. The execution time of the entire Mi task was 4 s. Subsequently, the subject continued to perform the next MI task. During the entire collection sequence, subjects were asked to maintain their bodies still and avoid blinking, eye movement, swallowing, or limb movements.

2.2 EEG data pre-processing

Pre-processing the EEG data extracted the time series covering the complete sequence of KMI events, that is, the entire 4 s period of prompting and executing each KMI task. An eight-order Butterworth band-pass filter was applied to remove noise interference and improve the signal-to-noise

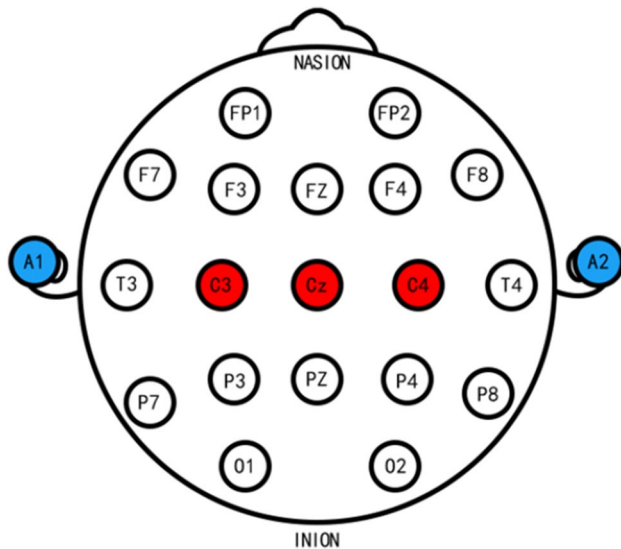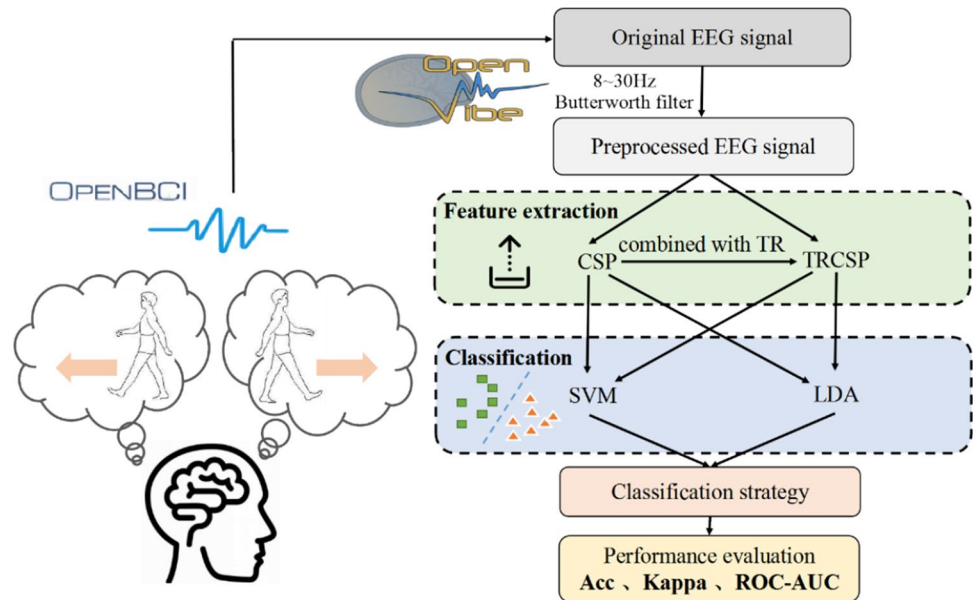**Fig. 1** Basic steps of research content

Fig. 2 Electrode placement according to 10–20 electrode system

ratio. The selected bandwidth range was 8–30 Hz because event-related desynchronisation and synchronisation (ERD/ERS) behaviour related to KMI, which primarily occurred in the mu (8–12 Hz) and beta (12–30 Hz) rhythms [25, 26].

2.3 TRCSP method for feature extraction

The EEG signal power filtered in a fixed frequency band corresponds to the signal variance. The CSP algorithm extracts the optimal features of the two types of MI EEGs based on band power features. Formally, the optimal spatial filter ω is designed by the simultaneous diagonalisation of two covariance matrices. The objective function is expressed as follows:

$$J(\omega) = \frac{\omega^T C_1 \omega}{\omega^T C_2 \omega} \tag{1}$$

where T denotes the transpose and C_1 and C_2 are the covariance matrices of classes 1 and 2, respectively.

However, it is necessary to regularise the CSP algorithm to overcome the sensitivity of the CSP algorithm to noise and overfitting. By adding a regularisation term to the objective function, we obtained the regularisation common spatial pattern (RCSP) algorithm. In particular, solutions that do not satisfy a given prior condition are penalised. In Eq. (2), $P(\omega)$ denotes the penalty function used to measure the degree to which the spatial filter ω satisfies the given prior condition. The more conditions ω satisfies, the smaller the value of $P(\omega)$. The TRCSP algorithm combines CSP with Tikhonov regularisation (TR). TR is a classical regularisation model, first introduced into regression problems to deal with penalty terms using weights. The penalty term $P(\omega)$ for the TRCSP algorithm is given as follows:

$$J(\omega) = \frac{\omega^T C_1 \omega}{\omega^T C_2 \omega + \alpha P(\omega)} \tag{2}$$

$$P(\omega) = \|\omega\|^2 = \omega^T \omega = \omega^T I \omega \tag{3}$$

where I represents the identity matrix. The regularisation parameter, α in Eq. (2), is the Tikhonov coefficient. A larger α implies a higher TR. With limited training data, or noise, the optimisation process of adjusting α can lead to

Fig. 3 Experimental paradigm
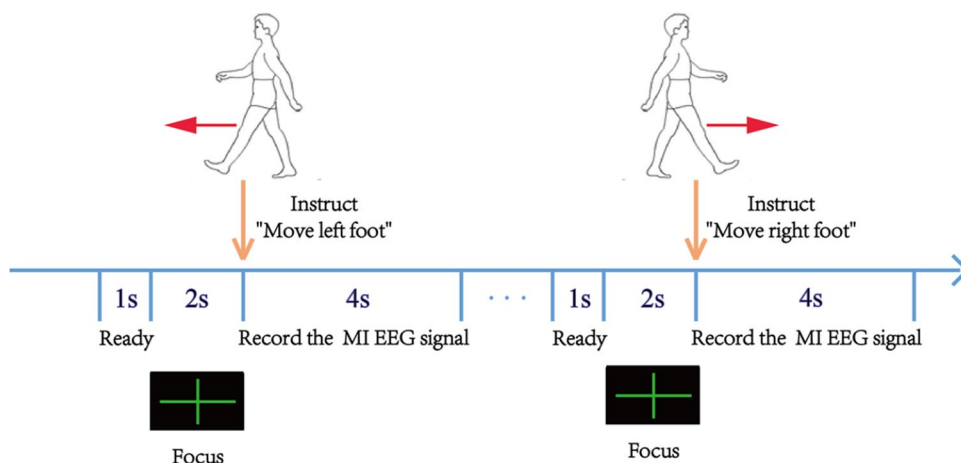
an effective spatial filter. Following numerous adjustment attempts, the parameter α was set to 3.

One advantage of TRCSP is that the new objective function is still a generalised eigenvalue problem, which can be solved by standard methods. However, adding the regularisation term eliminates the numerator–denominator symmetry in the objective function. Therefore, the eigenvalues should be determined twice to obtain the final spatial filter. Specifically, we must solve the following two objective functions:

$$J_1(\omega) = \frac{\omega^T C_1 \omega}{\omega^T C_2 \omega + \alpha \omega^T I \omega} \tag{4}$$

$$J_2(\omega) = \frac{\omega^T C_2 \omega}{\omega^T C_1 \omega + \alpha \omega^T I \omega} \tag{5}$$

Maximising $J_1(\omega)$ makes the variance of the first task the larger and that of the second task the smaller, while maximising $J_2(\omega)$ achieves the opposite. The eigenvector matrices obtained by solving the objective functions were $M_1 = (C_2 + \alpha I)^{-1} C_1$ and $M_2 = (C_1 + \alpha I)^{-1} C_2$. The eigenvector corresponding to the maximum eigenvalue was used to form the optimal spatial filter ω. The subsequent feature extraction method was the same as that of traditional CSP.

2.3.1 Classification

SVM and LDA have always been the most popular and practical classifiers for processing real-time EEG signals. We used binary SVM and LDA to combine with the spatial filtering algorithms TRCSP and CSP.

The goal of SVM is to map an input vector to high-dimensional feature space and construct the optimal classification hyperplane in this space to divide the feature vector into different classes. SVM has unique advantages in solving the problems of small-sample, nonlinear, and high-dimensional recognition [27]. We tested linear, nonlinear, and polynomial

kernel functions in the solution of the classification problem of the two KMI tasks. The linear kernel function performed best. Thus, we selected it as the final kernel function, and set the parameter C in support vector classification C-SVC to the value of one. A loss function known as SVM Hinge Loss was chosen to address the loss issue in SVM. The loss function is expressed as follows:

$$Hinge\ Loss = \sum_{i=1}^{n} 1 - d \tag{6}$$

where d is the distance from the sample point to the separating hyperplane and i is the number of samples between the support plane and the separating hyperplane. When the sample confidence meets the confidence interval and prediction interval is far less than the safety limit, the loss can be considered as 0. We obtained optimal separating hyperplane by adjusting parameters to calculate the loss minima of samples within the support plane and hyperplane, thus obtaining better binary classification results.

LDA provides good classification accuracy without high calculation costs [28]. Compared with the neural network algorithm, the LDA algorithm requires neither parameter adjustment nor weight optimisation. Moreover, LDA is not sensitive to the randomisation and normalisation of classification patterns. The principle of LDA is to reduce a high-dimensional problem to a low-dimensional problem by finding a projection direction. The transformed low-dimensional data must have minimum within-class and maximum between-class dispersion. We used the classic LDA algorithm with the setting to estimate the shrinkage coefficient automatically.

3 Results and analysis

To obtain better experimental results, we divided the data into training and testing sets in a ratio of 7:3. Using the TRCSP-SVM algorithm, the highest recognition accuracy

in the training set can approach 100%, and the lowest is 91.19%. The accuracy of training set is listed in Table 1. Then, the performances of testing set of the four algorithm combinations (TRCSP-SVM, TRCSP-LDA, CSP-SVM and CSP-LDA) were evaluated based on the accuracy, kappa coefficient, and ROC curve.

In the testing set, the highest recognition accuracy could reach 98.5%, the lowest was 96.43%, and the average recognition accuracy was 97.28% ± 0.97. For subjects S1 to S5, the accuracies of the four classification methods are listed in Table 2.

The kappa coefficient [29] is another important criterion used for the evaluation of classifier performance. In particular, the closer the value of kappa to one is, the more accurate the classification model. For subjects S1 to S5, the kappa coefficients for the four classification methods are shown in Table 3.

We also used ROC curves to quantify the performances of the classification combinations. The ROC curve is the probability curve for the true positive rate (TPR) (*y*-axis) versus the false positive rate (FPR) (*x*-axis) plotted using different thresholds. We defined the 'Move left foot' KMI as the positive class and 'Move right foot' KMI as the negative class. The area under the ROC curve (AUC) reflects the degree of separability between the two classes [30]. Typically, the higher the AUC is (in the range 0–1), the better the

classification performance, and the closer the ROC curve is to the upper left of the coordinate axes. For subjects S1 to S5, the ROC curves of the four classification methods are shown in Fig. 4, and the AUC values are listed in Table 4.

In summary, the TRCSP-SVM algorithm used in the lower limb KMI classification tasks achieved the best classification performance. Moreover, it exhibited a significant improvement compared with the standard CSP algorithm. We also compared our classification results with those of similar studies, as shown in Table 5. These results show that the TRCSP-SVM classification method used in this study is superior to other methods in several respects, such as average accuracy and AUC.

4 Discussion

Table 2 shows that the accuracy of all five subjects using TRCSP-SVM was higher than those obtained when other combinations were used. For example, compared with the average accuracy of the two combinations of CSP, those of TRCSP-SVM and TRCSP-LDA improved by 10% and 9%, respectively. Table 3 shows that for all four combination methods, kappa exceeded 0.5, showing high consistency. The average kappa coefficient of TRCSP-SVM was highest at 0.91. Compared with the two combination

Table 1 Accuracies of four classification methods (training set)

Method	Mean accuracy (%)	Subject				
		S1	S2	S3	S4	S5
TRCSP-SVM	99.02 ± 0.98	100.00	98.84	99.61	99.45	97.19
TRCSP-LDA	96.11 ± 1.05	96.74	94.44	96.31	97.52	95.54
CSP-SVM	93.33 ± 2.07	90.99	94.19	91.09	96.49	93.88
CSP-LDA	91.51 ± 2.59	90.05	89.98	90.11	90.73	96.67

Table 2 Accuracies of four classification methods (testing set)

Method	Mean accuracy (%)	Subject				
		S1	S2	S3	S4	S5
TRCSP-SVM	97.28 ± 0.97	98.50	97.17	96.24	98.04	96.43
TRCSP-LDA	92.79 ± 1.12	93.94	91.64	92.20	94.04	92.12
CSP-SVM	87.01 ± 3.13	84.38	90.76	83.28	89.00	87.63
CSP-LDA	83.33 ± 3.84	83.97	84.63	82.13	77.71	88.22

Table 3 Kappa coefficients of four classification methods (all subjects)

Method	Mean kappa	Subject				
		S1	S2	S3	S4	S5
TRCSP-SVM	0.91 ± 0.06	0.972	0.824	0.922	0.880	0.930
TRCSP-LDA	0.83 ± 0.04	0.878	0.814	0.842	0.782	0.842
CSP-SVM	0.74 ± 0.06	0.690	0.816	0.664	0.780	0.766
CSP-LDA	0.66 ± 0.08	0.680	0.692	0.636	0.548	0.752

(a)
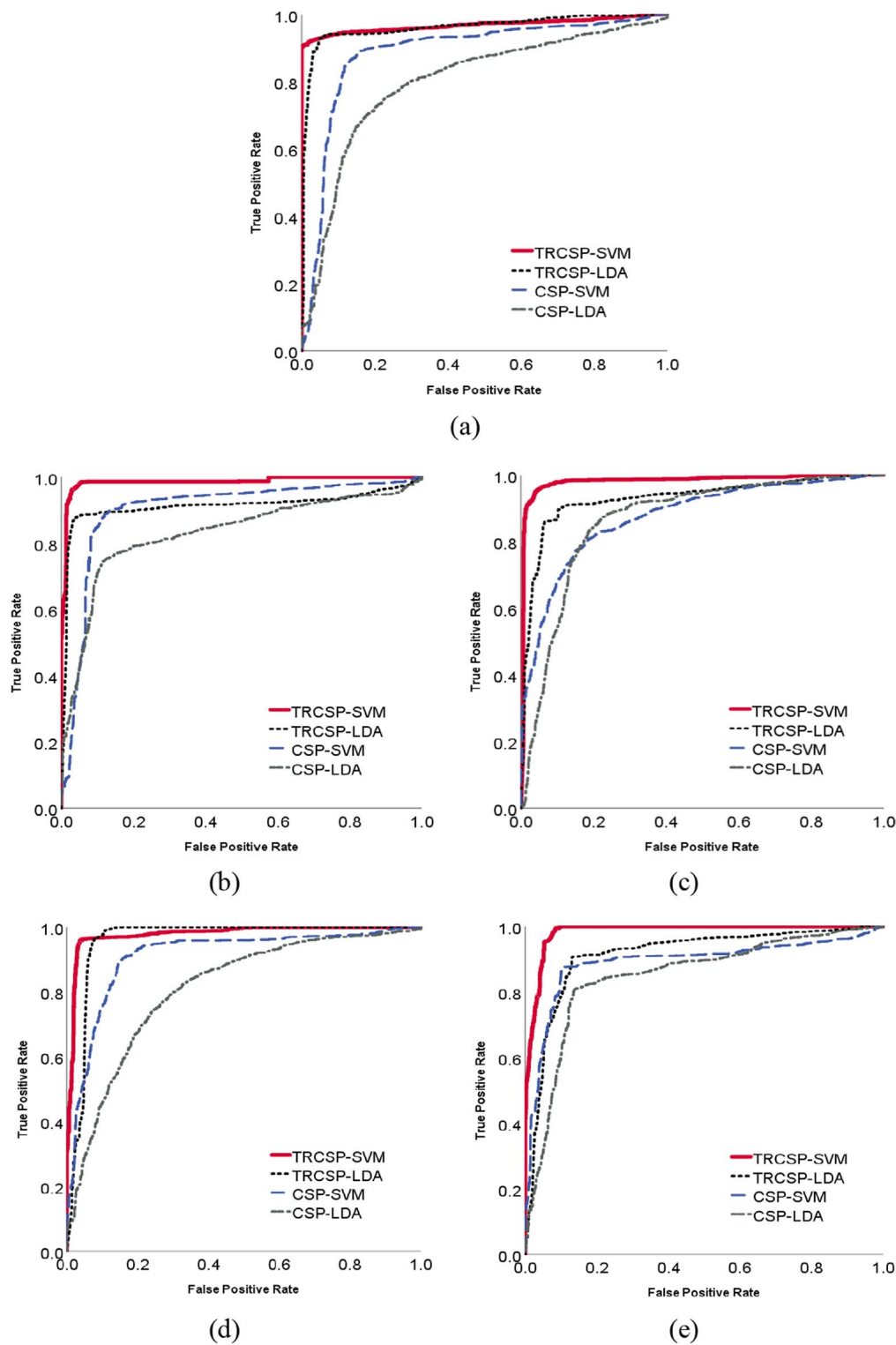

(b)

(c)

(d)

(e)

Fig. 4 ROC curves of the four classification methods, in which **a** to **e** correspond to subject S1 to S5 in turn

methods using CSP, the average kappa coefficient of the two methods using TRCSP increased by 0.17.

Figure 4 shows that the TRCSP-SVM method ROC curves of subjects S2, S3, and S5 are significantly better

than the other methods. Further, Table 4 shows that the average AUC value obtained by the TRCSP-SVM method is highest at 0.98. Compared with the average AUC of CSP-SVM, that of TRCSP-SVM improved by

Table 4 AUC values of four classification methods (all subjects)

Method	Mean AUC	Subject				
		S1	S2	S3	S4	S5
TRCSP-SVM	0.98 ± 0.01	0.968	0.986	0.981	0.978	0.984
TRCSP-LDA	0.94 ± 0.02	0.962	0.912	0.929	0.960	0.913
CSP-SVM	0.89 ± 0.01	0.888	0.902	0.876	0.911	0.891
CSP-LDA	0.83 ± 0.03	0.800	0.831	0.866	0.810	0.850

Table 5 Comparison with other related research results in literatures

Research work	Feature extraction	Classifier	Results (mean)		
			Accuracy (%)	Kappa	AUC
Fu et al. (2020) [18]	CSP	LDA	85.38		0.6947
	SCSP		94.13		0.8753
Dagdevir and Tokmakci (2021) [32]	CSP	SVM	96	0.91	
Li et al., 2021 [33]	FBCSP	SVM	78.59		0.7743
		LDA-KNN	84.62		0.8194
Cherloo et al. (2021) [34]	CSP	SVM	72.78		
	RCSP		77.28		
	RCSSP		78.07		
Tang et al. (2019) [21]	CSP	BPNN	86.17		
	B-CSP		90.43		
Our research methods	CSP	LDA	83.33	0.66	0.83
		SVM	87.01	0.74	0.89
	TRCSP	LDA	92.79	0.83	0.94
		SVM	97.28	0.91	0.98

approximately 0.1. Although the CSP-LDA method appeared relatively inappropriate based on the ROC curves of the five subjects, the AUC value reached 0.83, thus indicating that it can also achieve a relatively accurate classification. In addition, the AUC values obtained using the methods based on SVM were greater than those obtained using the methods based on LDA. The aforementioned accuracy and kappa coefficients reflect similar results. Our results show that the highest AUC value amongst the subjects did not correspond to the highest accuracy. Accuracy is calculated based on the best cut-off value, while AUC is based on all possible cut-off values, based on the integration of the prediction performance of all cut-off values. Thus, the accuracy can be high when the AUC value is not necessarily large and vice versa. The literature indicates that AUC is more robust than accuracy in model comparisons [31]. This is why we supplemented the accuracy with the ROC curve for evaluation and analysis.

However, the TRCSP + SVM algorithm and the TRCSP + LDA algorithm do not significantly differ in recognition accuracy, although their responses exhibits a substantial difference in the ROC curve. We decoded the classification results to gain insight into its causes and discovered that the SVM algorithm maximised and minimised the distance between the two classes of sample points reaching the hyperplane, resulting in a greater relative distance between the two classes of sample points. This is unlike the LDA algorithm, which only used the hyperplane to separate the two categories of sample points for binary classification. Thus, the ROC curve generated by the TRCSP + SVM algorithm is closer to the upper left corner, has a higher AUC value, and is more sensitive.

Most BCI models require subject-specific training, and it is time-consuming and costly to collect subject-specific training data for every new user. Although the TRCSP + SVM algorithm has shown advantages in the lower limb kinaesthetic motor imagery classification task, the cross-subject performance is still unknown. Therefore, in the next stage, we plan to investigate the cross-subject problem in the hope of finding a more suitable cross-subject method.

5 Conclusions

We investigated four algorithm combinations to optimise the classification strategy and performance of an MI-BCI system by distinguishing left and right foot movements. These combinations were TRCSP-SVM, TRCSP-LDA, CSP-SVM, and CSP-LDA. The TRCSP algorithm was used to extract brain signal features, while noise sensitivity and overfitting associated with the traditional CSP algorithm were reduced. Methods which used the TRCSP algorithm outperformed methods which were based on the CSP algorithm. In particular, the average accuracy increased by 9–10%, the average kappa coefficient increased by 0.17, and the average AUC value increased by approximately 0.1. Moreover, our results showed that the SVM classifier performed significantly better than LDA. Therefore, as the best combination of spatial filtering and classification algorithms, the TRCSP-SVM method shows a great potential for improving the performance of lower limb KMI systems. Our results provide not only new ideas for the optimisation of algorithmic strategies but also promising opportunities for the realisation of 'what you think is what you move' approach in lower limb rehabilitation training.

Declarations

Consent to participate Before the experiment, all subjects signed the informed written consent and agreed to participate in this experiment.

Competing interests The authors declare no competing interests.

References

1. Attallah O, Abougharbia J, Tamazin M, Nasser AA (2020) A BCI system based on motor imagery for assisting people with motor deficiencies in the limbs. Brain Sci 10:864. https://doi.org/10.3390/brainsci10110864

2. Kraus D, Naros G, Bauer R et al (2016) Brain–robot interface driven plasticity: distributed modulation of corticospinal excitability. Neuroimage 125:522–532. https://doi.org/10.1016/j.neuroimage.2015.09.074

3. Simon C, Bolton DAE, Kennedy NC et al (2021) Challenges and opportunities for the future of brain-computer interface in neurorehabilitation. Front Neurosci 15:1–8. https://doi.org/10.3389/fnins.2021.699428

4. Bhattacharyya S, Konar A, Tibarewala DN (2014) A differential evolution based energy trajectory planner for artificial limb control using motor imagery EEG signal. Biomed Signal Process Control 11:107–113. https://doi.org/10.1016/j.bspc.2014.03.001

5. Wang X, Lu H, Shen X et al (2021) Prosthetic control system based on motor imagery. Comput Methods Biomech Biomed Eng 0:1–8 https://doi.org/10.1080/10255842.2021.1977800

6. Ono Y, Wada K, Kurata M, Seki N (2018) Enhancement of motor-imagery ability via combined action observation and motor-imagery training with proprioceptive neurofeedback. Neuropsychologia 114:134–142. https://doi.org/10.1016/j.neuropsychologia.2018.04.016

7. Liang S, Choi K-S, Qin J et al (2016) Improving the discrimination of hand motor imagery via virtual reality based visual guidance. Comput Methods Programs Biomed 132:63–74. https://doi.org/10.1016/j.cmpb.2016.04.023

8. Rahman MA, Khanam F, Ahmad M, Uddin MS (2020) Multiclass EEG signal classification utilizing Rényi min-entropy-based feature selection from wavelet packet transformation. Brain Informatics 7:1–11. https://doi.org/10.1186/s40708-020-00108-y

9. Mohamed AMA, Uçan ON, Bayat O, Duru AD (2020) Classification of resting-state status based on sample entropy and power spectrum of electroencephalography (EEG). Appl Bionics Biomech 2020:1–10. https://doi.org/10.1155/2020/8853238

10. Kim C, Sun J, Liu D et al (2018) An effective feature extraction method by power spectral density of EEG signal for 2-class motor imagery-based BCI. Med Biol Eng Comput 56:1645–1658. https://doi.org/10.1007/s11517-017-1761-4

11. Khalaf A, Sejdic E, Akcakaya M (2019) Common spatial pattern and wavelet decomposition for motor imagery EEG-fTCD brain-computer interface. J Neurosci Methods 320:98–106. https://doi.org/10.1016/j.jneumeth.2019.03.018

12. Chacon-Murguia MI, Olivas-Padilla BE, Ramirez-Quintana J (2020) A new approach for multiclass motor imagery recognition using pattern image features generated from common spatial patterns. SIViP 14:915–923. https://doi.org/10.1007/s11760-019-01623-0

13. Aldea R, Fira M (2014) Classifications of motor imagery tasks in brain computer interface using linear discriminant analysis. International Journal of Adv Res Artif Intell 3:5–9.https://doi.org/10.14569/IJARAI.2014.030702

14. Shen X, Wang X, Lu S, et al (2022) Research on the real-time control system of lower-limb gait movement based on motor imagery and central pattern generator. Biomed Signal Process Control 71:102803 https://doi.org/10.1016/j.bspc.2021.102803

15. Djoufack Nkengfack LC, Tchiotsop D, Atangana R, et al (2020) EEG signals analysis for epileptic seizures detection using polynomial transforms, linear discriminant analysis and support vector machines. Biomed Signal Process Control 62:102141 https://doi.org/10.1016/j.bspc.2020.102141

16. Petersen J, Iversen HK, Puthusserypady S (2018) Motor imagery based brain computer interface paradigm for upper limb stroke rehabilitation. In: 2018 40th Annual International Conference of the IEEE Engineering in Medicine and Biology Society (EMBC). IEEE, pp 1960–1963. https://doi.org/10.1109/EMBC.2018.8512615

17. Rani Alex JS, Haque MA, Anand A et al (2020) A deep learning approach for robotic arm control using brain-computer interface. Int J Biol Biomed Eng 14:128–135 https://doi.org/10.46300/91011.2020.14.18

18. Fu R, Han M, Tian Y, Shi P (2020) Improvement motor imagery EEG classification based on sparse common spatial pattern and regularized discriminant analysis. J Neurosci Methods 343:108833 https://doi.org/10.1016/j.jneumeth.2020.108833

19. Shuaibu Z, Qi L (2020) Optimized DNN classification framework based on filter bank common spatial pattern (FBCSP) for motor-imagery-based BCI. Int J Comput Applic 175:16–25. https://doi.org/10.5120/ijca2020920646

20. AnaP C, JakobS M, HelleK I, Puthusserypady S (2018) An adaptive CSP filter to investigate user independence in a 3-class MI-BCI paradigm. Comput Biol Med 103:24–33. https://doi.org/10.1016/j.compbiomed.2018.09.021

21. Tang Z, Li C, Wu J et al (2019) Classification of EEG-based single-trial motor imagery tasks using a B-CSP method for BCI. Front Inform Technol Electron Eng 20:1087–1098. https://doi.org/10.1631/FITEE.1800083

22. Lu, Z., Zhang X et al (2022) An asynchronous artifact-enhanced electroencephalogram based control paradigm assisted by slight facial expression. Front neurosci 16:892794 https://doi.org/10.3389/fnins.2022.892794

23. Zhang, X., Lu Z et al (2021) Realizing the application of EEG modeling in BCI classification: based on a conditional GAN converter. Front Neurosci 15:727394 https://doi.org/10.3389/fnins.2021.727394

24. Jin J, Miao Y, Daly I et al (2019) Correlation-based channel selection and regularized feature optimization for MI-based BCI. Neural Netw 118:262–270. https://doi.org/10.1016/j.neunet.2019.07.008

25. Wang Z, Yu Y, Xu M et al (2019) Towards a hybrid BCI gaming paradigm based on motor imagery and SSVEP. Int J Hum-Comput Interact 35:197–205. https://doi.org/10.1080/10447318.2018.1445068

26. Lotte F, Guan C (2011) Regularizing common spatial patterns to improve BCI designs: unified theory and new algorithms. IEEE Trans Biomed Eng 58:355–362. https://doi.org/10.1109/TBME.2010.2082539

27. Ghumman MK, Singh S, Singh N, Jindal B (2021) Optimization of parameters for improving the performance of EEG-based BCI system. J Reliable Intell Environ 7:145–156. https://doi.org/10.1007/s40860-020-00117-y

28. Li Y, Koike Y (2011) A real-time BCI with a small number of channels based on CSP. Neural Comput Appl 20:1187–1192. https://doi.org/10.1007/s00521-010-0481-6

29. Jusas S (2019) Classification of motor imagery using a combination of user-specific band and subject-specific band for brain-computer interface. Appl Sci 9:9–10. https://doi.org/10.3390/app9234990

30. Tariq M, Trivailo PM, Simic M (2019) Classification of left and right knee extension motor imagery using common spatial pattern for BCI applications. Procedia Comput Sci 159:2598–2606. https://doi.org/10.1016/j.procs.2019.09.256

31. Ling CX, Huang J, Zhang H (2003) AUC: a better measure than accuracy in comparing learning algorithms. In: Lecture Notes in Computer Science (including subseries Lecture Notes in Artificial Intelligence and Lecture Notes in Bioinformatics), pp 329–341. https://doi.org/10.1007/3-540-44886-1_25

32. Dagdevir E, Tokmakci M (2021) Truncation thresholds based empirical mode decomposition approach for classification performance of motor imagery BCI systems. Chaos Solitons Fractals 152:111450 https://doi.org/10.1016/j.chaos.2021.111450

33. Jia Ying Li;Li Zhao;Yan Bian (2021) Classification of lower limb motor imagination signals based on LDA and KNN. Foreign Electron Meas Technol 40:9–14. https://doi.org/10.19652/j.cnki.femt.2002388

34. Norizadeh Cherloo M, Kashefi Amiri H, Daliri MR (2021) Ensemble regularized common spatio-spectral pattern (ensemble RCSSP) model for motor imagery-based EEG signal classification. Comput Biol Med 135:104546 https://doi.org/10.1016/j.compbiomed.2021.104546

Jiakai Zhang was born in 1998. He is a postgraduate student at the School of Information Science and Technology of Nantong University. His research interests are in the acquisition of biological signals and information processing, brain–computer interface, and EEG signals acquisition and classification.
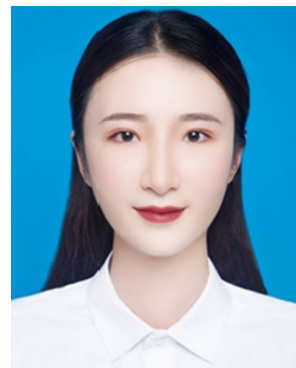
Xuemei Wang was born in 1996. She is a postgraduate student at the School of Information Science and Technology of Nantong University. Her research interests are in the acquisition of biological signals and information processing, biomedical electronics, and biomedical engineering.
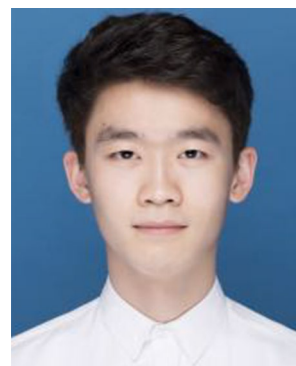
Boyang Xu was born in 1999. He is a postgraduate student at the School of Information Science and Technology of Nantong University. His research interests are biomedical electronics and Bluetooth RSSI ranging system.

Yan Wu was born in 1997. She is a postgraduate student at the School of Information Science and Technology of Nantong University. Her research interest is biological signal tracking and processing.

Xiongjie Lou was born in 1998. He is a postgraduate student at the School of Information Science and Technology of Nantong University. His research interest is biological signal control.

Xiaoyan Shen was born in 1969. She is a PhD, professor, and PhD supervisor. She is a high-level talent training target of 'Six Talents' Peaks' in Jiangsu Province and a second-level young and middle-aged science and technology leading talents of Nantong City '226' Project. She is a backbone of Jiangsu Nerve Regeneration Coordination Innovation Center and a member of the Rehabilitation Education Professional Committee of Nantong Rehabilitation Medicine Association. She is a leader of Medical Information Technology in Information and Communication Engineering, School of Information Science and Technology, Nantong University. She mainly engaged in biological neural interface technology, neural signal detection circuit and functional electrical excitation circuit design, neural signal and electromyographic signal acquisition technology and analysis, neural signal regeneration, and functional reconstruction.